Ultrafast observation of lattice dynamics in laser-irradiated gold foils

N. J. Hartley, N. Ozaki, T. Matsuoka, B. Albertazzi, A. Faenov, Y. Fujimoto, H. Habara, M. Harmand, Y. Inubushi, T. Katayama, M. Koenig, A. Krygier, P. Mabey, Y. Matsumura, S. Matsuyama, E. E. McBride, K. Miyanishi, G. Morard, T. Okuchi, T. Pikuz, O. Sakata, Y. Sano, T. Sato, T. Sekine, Y. Seto, K. Takahashi, K. A. Tanaka, Y. Tange, T. Togashi, Y. Umeda, T. Vinci, M. Yabashi, T. Yabuuchi, K. Yamauchi, and R. Kodama

Citation: Appl. Phys. Lett. **110**, 071905 (2017); doi: 10.1063/1.4976541
View online: http://dx.doi.org/10.1063/1.4976541
View Table of Contents: http://aip.scitation.org/toc/apl/110/7
Published by the American Institute of Physics

Ultrafast observation of lattice dynamics in laser-irradiated gold foils

N. J. Hartley,[1,2,a)] N. Ozaki,[2,3,b)] T. Matsuoka,[4] B. Albertazzi,[2,5] A. Faenov,[4,6] Y. Fujimoto,[2] H. Habara,[2,3] M. Harmand,[7] Y. Inubushi,[8] T. Katayama,[8] M. Koenig,[2,5] A. Krygier,[7] P. Mabey,[9] Y. Matsumura,[2] S. Matsuyama,[2] E. E. McBride,[10] K. Miyanishi,[2] G. Morard,[7] T. Okuchi,[11] T. Pikuz,[2,6] O. Sakata,[12] Y. Sano,[2] T. Sato,[13] T. Sekine,[13] Y. Seto,[14] K. Takahashi,[2,3] K. A. Tanaka,[2,3] Y. Tange,[8] T. Togashi,[8] Y. Umeda,[13] T. Vinci,[5] M. Yabashi,[15] T. Yabuuchi,[15] K. Yamauchi,[2] and R. Kodama[2,3,4,16]

[1]*Helmholtz-Zentrum Dresden-Rossendorf, Dresden 01328, Germany*
[2]*Graduate School of Engineering, Osaka University, Suita, Osaka 565-0871, Japan*
[3]*Photon Pioneers Center, Osaka University, Suita, Osaka 565-0871, Japan*
[4]*Institute for Academic Initiatives, Osaka University, Suita, Osaka 565-0871, Japan*
[5]*LULI, CNRS, Ecole Polytechnique, 91128 Palaiseau Cedex, France*
[6]*Joint Institute for High Temperatures, Russian Academy of Sciences, Moscow 125412, Russia*
[7]*IMPMC Institut de Minéralogie, de Physique des Matériaux et de Cosmochimie, UPMC, CNRS, MNHN, IRD, 75005 Paris, France*
[8]*Japan Synchrotron Radiation Research Institute, Sayo, Hyogo 679-5198, Japan*
[9]*Department of Physics, University of Oxford, Oxford OX1 3PU, United Kingdom*
[10]*SLAC National Accelerator Laboratory, Menlo Park, California 94025, USA*
[11]*Institute for Planetary Materials, Okayama University, Tottori 682-0193, Japan*
[12]*Synchrotron X-ray Station at SPring-8, National Institute for Materials Science, Sayo, Hyogo 679-5148, Japan*
[13]*Graduate School of Science, Hiroshima University, Higashi-Hiroshima 739-8526, Japan*
[14]*Graduate School of Science, Kobe University, Kobe, Hyogo 657-8501, Japan*
[15]*RIKEN Spring-8 Center, Sayo, Hyogo 679-5148, Japan*
[16]*Institute of Laser Engineering, Osaka University, Suita, Osaka 565-0871, Japan*

(Received 11 January 2017; accepted 24 January 2017; published online 17 February 2017)

We have observed the lattice expansion before the onset of compression in an optical-laser-driven target, using diffraction of femtosecond X-ray beams generated by the SPring-8 Angstrom Compact Free-electron Laser. The change in diffraction angle provides a direct measure of the lattice spacing, allowing the density to be calculated with a precision of $\pm 1\%$. From the known equation of state relations, this allows an estimation of the temperature responsible for the expansion as <1000 K. The subsequent ablation-driven compression was observed with a clear rise in density at later times. This demonstrates the feasibility of studying the dynamics of preheating and shock formation with unprecedented detail. *Published by AIP Publishing.* [http://dx.doi.org/10.1063/1.4976541]

The advent of X-ray free electron lasers (XFELs) has allowed unparalleled insight into the behaviour of solid materials on the timescales of atomic motion, with a greater fidelity than had been possible with previous techniques.[1,2] This has applications in areas such as materials science,[3,4] high energy density physics,[5,6] and planetary science[7,8] among others. Likewise, laser driven dynamic compression has been used to study materials under extreme conditions for scientific and engineering applications. By combining these, XFEL-XRD (X-ray Diffraction) observations can provide much greater detail than had previously been possible,[9] probing ultrafast lattice-level dynamical phenomena and transient states associated with shock compression including laser ablation, shock formation, and phase transformations which are all difficult to predict with only simulations. Such results are of interest not just for basic science research, but also for work on laser processing such as peening.[10]

In this letter, we report on femtosecond XFEL-XRD observations of lattice dynamics in gold targets irradiated by a sub-nanosecond optical laser pulse. Gold is an ideal substance for observing these dynamics and is commonly used for high energy density experiments, including as an X-ray hohlraum,[11,12] and for static high pressure experiments as a pressure standard in the solid phase regime.[13] Its equation of state (EOS) is well-known up to 100 s of GPa and has no phase transformations reported, allowing conditions to be deduced from XRD measurements, even in dynamic high-pressure experiments.[14,15]

This experiment was performed at the SACLA (SPring-8 Angstrom Compact Free-electron Laser) facility.[16] As shown in the schematic in Fig. 1(a), a 500 nm thick polycrystalline gold foil coating deposited on a 100 μm thick acrylic substrate was illuminated by an 800 nm wavelength laser at an average intensity of $\sim 2.5 \times 10^{12}$ W/cm^2, with $\sim$1 J in 660 ps focused onto a 280 μm FWHM spot. The intensity was estimated on-shot from temperature measurements of the coronal plasma,[17] and the temporal shape was quasi-trapezoidal with a rise time of $\sim$200 ps. The contrast between the peak intensity and the pedestal of the laser pulse was better than 10^{-5}. The sample was probed from the reverse (non-laser) side by a 7 fs quasi-monochromatic (bandwidth 0.25%) X-ray pulse at an energy of $\sim$10 keV

a)n.hartley@hzdr.de
b)norimasa.ozaki@eei.eng.osaka-u.ac.jp

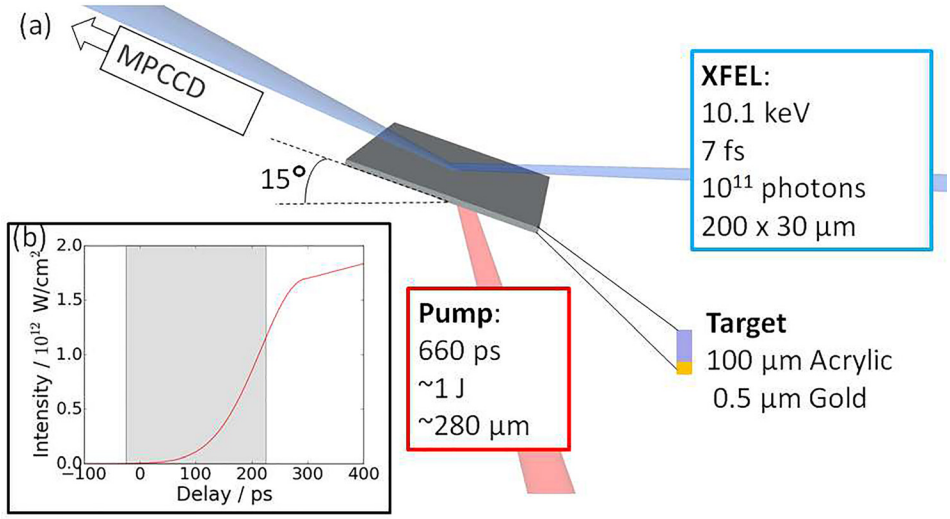

FIG. 1. (a) Schematic of experimental setup inside vacuum target chamber. The polycrystalline gold target is illuminated by an optical ($\lambda = 800$ nm) pump laser. The lattice spacing of the target is probed by the ultrafast XFEL beam from the opposite side, with the diffracted signal measured on the MPCCD detector outside the vacuum chamber. (b) Approximate pump pulse waveform, with probed delays shaded.

with $\sim 10^{11}$ photons per pulse. The beam was line focused in the vertical axis to 30 μm using a Kirkpatrick-Baez (KB) mirror, with the other axis adjusted to a width of 200 μm using a two-quadrant slit. The target was placed at an angle of 15° relative to the XFEL beam axis, thereby probing the lattice d-spacing in reflection geometry. With an attenuation length of ~ 1 μm X-rays probe the full depth of the foil, allowing us to observe the dynamics of the laser-matter interaction at the earliest times. Arcs of the (111) and (200) Debye-Scherrer rings were observed at 2θ angles of 30.2° and 35.0°, respectively, on a one-megapixel array detector (MPCCD) located outside the vacuum chamber at a distance of ~ 30 cm from the sample, and visible through a Kapton window. The pump-probe delay was varied to observe the evolution of the lattice spacing within the sample from the onset of illumination.

The initial Au grains are uniform in size, estimated from the Scherrer Equation[18] as around 20 nm, and randomly orientated, as confirmed by XRD measurements using a synchrotron source before the experiment, and before each data shot at the XFEL. The initial density was 19.24 g/cc, within the range expected at standard pressure and temperature conditions. Since the Hugoniot elastic limit in gold is too low to be detected in shock experiments, the sample is suitable for achieving isotropic (hydrostatic) compression and expansion conditions.

Examples of the observed data are shown in Fig. 2 with the (111) and (200) diffraction lines visible. Data from the initial ambient matter is seen in Fig. 2(a); in the later shots, shown in Figs. 2(b)–2(f), data is seen at both higher and lower angles than the initial line, denoting the presence of matter at higher and lower densities, respectively.

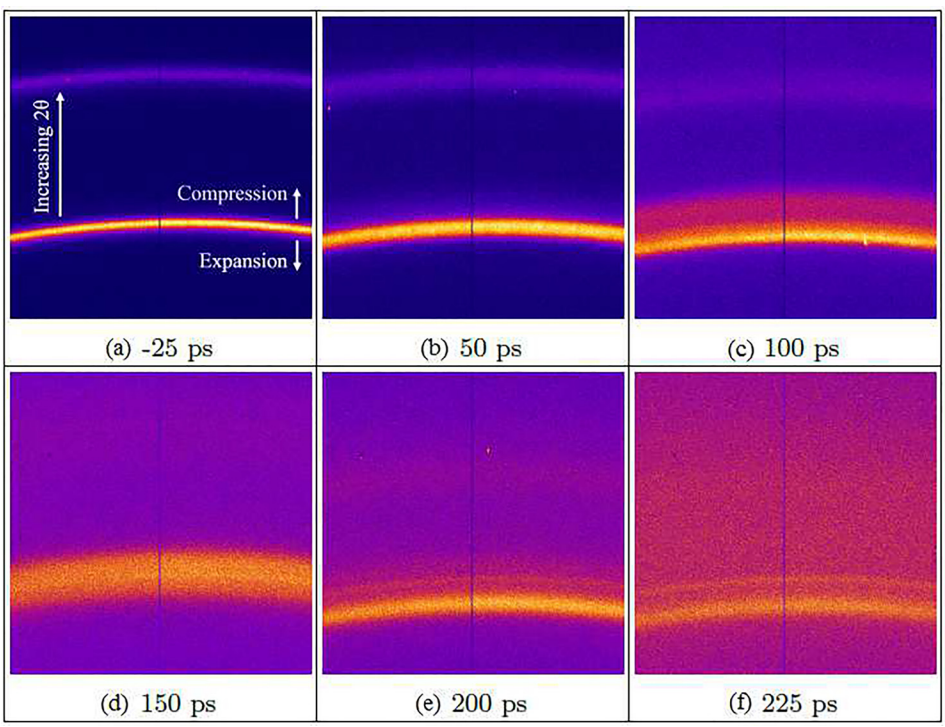

FIG. 2. Diffraction patterns obtained on the MPCCD at different pump-probe delays, showing the angular deviation of the diffracted X-rays due to changes in the lattice spacing d. The visible lines are (lower) (111)@30.2° and (upper) (200)@35.2° $t = 0$ is defined at the foot of the drive laser pulse. Shots taken at later times showed no diffraction signal. The color scale is consistent across the different delays.

In Figs. 2(a)–2(c) we can see that the lines broaden, due to sample heating, and shift to lower angles, corresponding to an expansion in the sample. This appears to be due to the low laser intensity, $<10^{11}\,\mathrm{W/cm^2}$, only moderately heating the target, such that it remains a solid but expands due to the rise in temperature. At later times, the intensity has increased sufficiently to start ablating the sample and drive a compression wave, with signal from compressed matter seen in Figs. 2(c) and 2(d). After this compression reaches the acrylic substrate, a rarefaction wave passes back into the gold due to the large impedance mismatch, so that we again see matter at lower than initial densities in Figs. 2(e) and 2(f). Although this is still early in the laser pulse, there was no diffraction signal at later times because the compressed matter is rarefied by the reflected wave.

Such details of laser ablation and shock formation, and the dynamics within the compression front, are resolved on XFEL systems such as this with unmatched precision, compared to laser-driven X-ray sources. The XFEL provides a highly collimated ($\sim 2\,\mu$rad) and narrow band ($\sim 0.5\,$eV) probe beam, giving resolution limited only by the monocrystallinity of the sample. This allows observation of complex behaviour just before and within the compression front, and experiments such as this are crucial for better understanding a regime where theoretical models are few, and often inaccurate.

Although there are no direct temperature diagnostics in this experiment, we can estimate the temperature in the sample using an equation of state (EOS) such as the Rose-Vinet EOS,[19] which remains valid while the target is still solid, and has previously been used to good effect with gold.[20] The EOS parameters are taken from Yokoo *et al.*,[13] and are chosen to agree with the experimental results over a range of temperature and pressure conditions. Although XRD experiments such as this are often able to use the Debye-Waller effect to estimate the temperature, the signal strength in this experiment is dominated by the density distribution, rather than the temperature. As this distribution is not accurately known, we are not able to estimate the temperature in this way.

Fig. 3 shows the results of a one-dimensional radiation hydrodynamics simulation of the sample evolution due to the incident laser pulse.[21] The early part of the pulse, with intensity $<10^{11}\,\mathrm{W/cm^2}$, heats the electrons in a thin region close to the surface,[22] which rapidly equilibrate with the ions,[23,24] causing the foil to expand isotropically. This increase in temperature propagates through the target by conduction, with an associated reduction in density. Subsequently, the intensity reaches a sufficient level to start strongly ablating the sample,[25] launching a compression wave.

Considering the behaviour more quantitatively, we look at lineouts across the (111) diffraction peak, shown in Fig. 4. The lineouts are well reproduced by a three-Gaussian fit (one each for matter at initial, lower, and higher densities). Data from the (200) diffraction peak gives comparable results for the changes in peak positions and relative heights, although with less confidence due to the lower signal/noise ratio. We see in Fig. 4(a) that a peak from expanded matter, to the left of the original line, is present and separated from the initial θ_0 peak by $0.16 \pm 0.1°$; from Bragg's law, this implies a

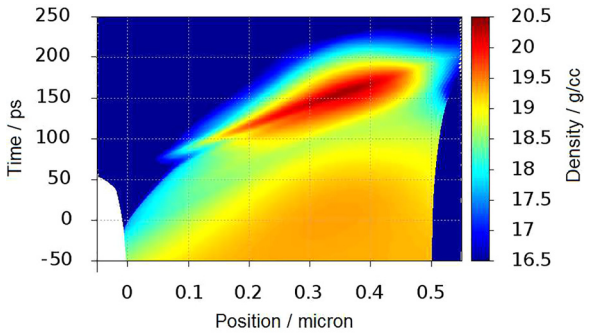

FIG. 3. Evolution of the sample density due to the incident laser pulse from Figure 1(b), simulated with the 1-D radiation hydrodynamics code Multi, using Sesame EOS 2700. The simulation starts at earlier times to include the effects of heating by the early part of the pulse.

change in the lattice spacing of $\Delta d/d_0 = 0.5 \pm 0.3\%$. Since the heating is not a directed process, we assume that the behaviour is isotropic, and that this therefore corresponds to a volume change $\Delta V/V_0 = 1.5 \pm 1.0\%$ and an absolute density of $18.9 \pm 0.2\,$g/cc. When the material is heated at ambient pressures, the temperature needed to explain the expansion can be calculated using the coefficient of thermal expansion, β,[26] giving $650 \pm 210\,$K.

Analysis of the lineouts for expanded matter in Fig. 4(b) ($t = 62$ ps) and Fig. 4(c) ($t = 125$ ps) gives densities of 18.6 ± 0.2 and $18.4 \pm 0.2\,$g/cc, similar to the densities seen in the simulation in Fig. 3. The corresponding temperatures

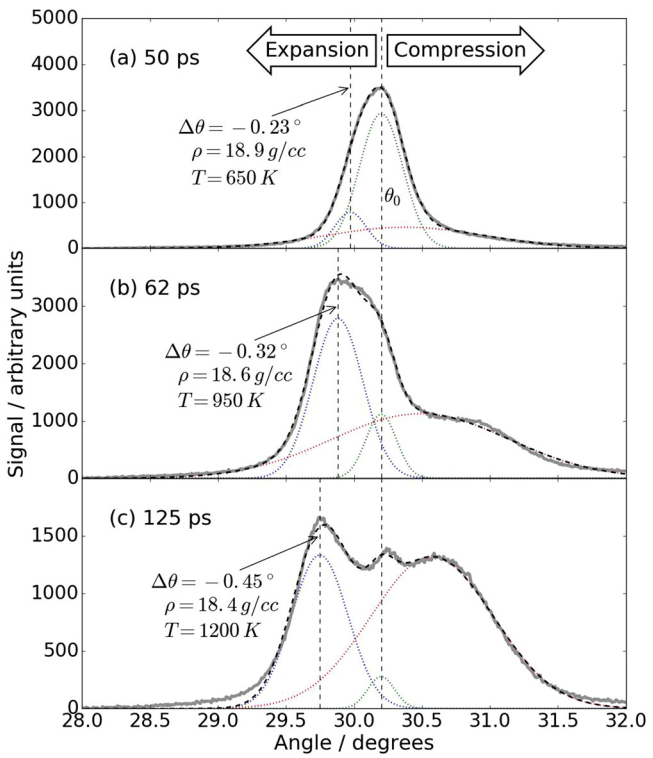

FIG. 4. Lineouts, in grey, of the (111) diffraction line averaged across the MPCCD from single shots, at various delays from the foot of the drive laser pulse. The dotted lines indicate Gaussian fits to the data. The RMS differences between the Gaussian fits and experimental data are 17.5, 35.9, and 30.3 for (a), (b), and (c) respectively. Densities and temperatures of the expanded peaks are calculated assuming isotropic compression and the Rose-Vinet EOS, respectively.

calculated with β are 950 ± 200 and 1200 ± 200 K, respectively. The line widths of these expanded peaks are comparable to those of the cold Au samples throughout the sample evolution, indicating that the expanded matter is characterized by a single lattice spacing at each time, and that therefore the temperature of the heated region is approximately uniform.

In this experiment, the preheating is due to the long ($\sim$200 ps) rise time of the laser, the rapid heat exchange between the electrons and ions and the high thermal conductivity of gold (318 $W/m \cdot K$). However, the same techniques are applicable for preheating from any source. In experiments with a low laser contrast, prepulses often heat the sample, affecting the subsequent shock formation. Similarly, radiation from the coronal plasma in shock compression experiments and equation of state studies can heat the region ahead of the shock, possibly influencing the accuracy of the results. While such effects are not always easy to model, these results demonstrate the feasibility of directly monitoring them in experiments and better understanding preshock dynamics in samples.

Turning to the $\theta > \theta_0$ region in Fig. 4, these show that from a delay of 62 ps onwards, the sample contains significant amounts of compressed matter due to the pressure from the laser ablation. In contrast to the narrow peak from the expanded matter, the signal is consistently very broad, indicating the presence of multiple lattice spacings and implying that a ramp compression wave with a significant density gradient is driven after the expansion. The states at these early times are therefore not located on the Principal Hugoniot.

The highest density (smallest volume compression) observed was 20.6 ± 0.3 g/cc (0.937 ± 0.013), in very good agreement with the Multi simulation. Looking at the phase diagram in Fig. 5, we can estimate the pressure and temperature required for this compression in the sample. The measured density gives an isochore in temperature-pressure space, shown as the dashed line, estimated from EOS of Yokoo *et al.*[13] The temperature before compression begins, estimated from the expansion, is shown as a shaded region,

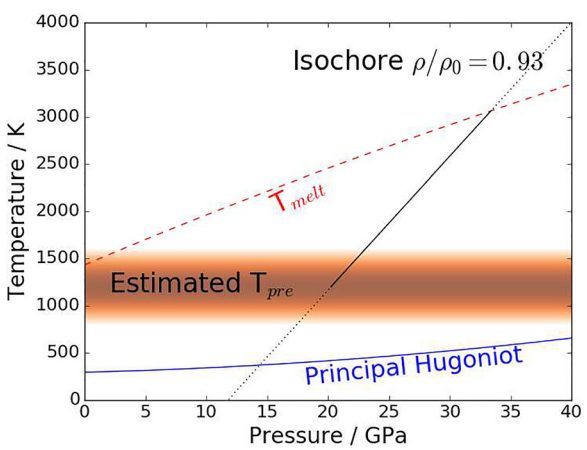

FIG. 5. Region of gold phase diagram; pressure dependent melting temperature T_{melt} (red dashed line) from Ref. 26, temperature before the shock T_{pre} (shaded region, indicating uncertainty) estimated as above, principal Hugoniot from Sesame (blue solid line). Black line gives states corresponding to the observed compression in the RVEOS, using parameters from Ref. 13; solid indicates states possible here (between T_{pre} and T_{melt}).

meaning that the possible states for the compressed material are along the isochore, between the initial and melting temperatures. The temperature of these states is much higher than what would be found along the principal Hugoniot for gold, shown as the lower solid line in Fig. 5.

The rapid growth of the compressed region with time agrees with the compression wave traveling faster than the prior thermal expansion front. Once it overtakes the thermal front, it would, in a thicker target, coalesce into a single shock wave with thermodynamic states located on the Hugoniot, as it would then be moving into cold material instead of the preheated sample. These results do show that this experimental setup is ideally suited to observing shock formation behaviour, and that performing similar experiments with a thicker target or faster rise time to give shock, rather than ramped, compression will allow increased understanding of the behaviour of this phenomena.

Overall, the agreement of the hydrodynamic simulation in Fig. 3 with the observed data is good. The simulation already shows significant heating by $t = 0$, due to the laser rise time, although the signal remains dominated by the diffraction from the large amount of cold material. By 50 ps, the expansion wave has propagated further through the sample and is visible in the diffraction data in Fig. 4(a). By 100 ps, the clear compressed peak seen in Fig. 2(c) begins to appear in the simulation, driven by the ablation at the laser surface, and by 125 ps, shown in Fig. 4(c), the compressed and expanded regions have similar sizes. The compression signal is not seen at all from 200 ps onwards, as the compression wave has broken out into the plastic substrate. The remaining signal from the expanded lattice rapidly weakens, as seen in Fig. 2(f), and latter times show no coherent signal.

In conclusion, we have observed the lattice level shock formation phenomena at the earliest stages of laser irradiation. Diffraction of an XFEL beam allows a direct measurement of the lattice spacing, and therefore the density of the sample, with a precision of 1%. This shows lattice expansion, which simulations show to be ahead of the compression wave, and is able to resolve the compression due to increasing pressure in the sample before the formation of the shock. The well understood equation of state also allows an estimate of the temperature in the material and would therefore be suitable for laser shock experiments, as it is able to estimate much lower temperatures than are accessible with the widely used streaked optical pyrometers. The method presented here is sensitive to changes in the temperature of <1000 K while also having an exceptional time resolution.

The authors would like to thank Y. Kimura for her support with target fabrication. The XFEL experiments were performed at the BL3 of SACLA with the approval of the Japan Synchrotron Radiation Research Institute (JASRI) (Proposal Nos. 2012A8015, 2012B8015, 2012B8046, 2013B8063, 2014A8045, 25707041, and 2015A8066). This work was supported in part by JSPS KAKENHI (Grant Nos. 16K17846, 15K13609, and 15H05751), JSPS core-to-core program on International Alliance for Material Science in Extreme States with High Power Laser and XFEL, the X-ray Free Electron Laser Priority Strategy Program at Osaka University from the Ministry of Education, Culture, Sports, Science and

Technology (MEXT), under Contract No. 12005014 and the French Agence Nationale de la Recherche (ANR) with ANR IRONFEL 12-PDOC-0011. E.E.M. acknowledges funding from the Volkswagen Foundation.

[1]M. G. Gorman, R. Briggs, E. E. McBride, A. Higginbotham, B. Arnold, J. H. Eggert, D. E. Fratanduono, E. Galtier, A. E. Lazicki, H. J. Lee, H. P. Liermann, B. Nagler, A. Rothkirch, R. F. Smith, D. C. Swift, G. W. Collins, J. S. Wark, and M. I. McMahon, "Direct observation of melting in shock-compressed bismuth with femtosecond X-ray diffraction," Phys. Rev. Lett. **115**, 095701 (2015).
[2]G. B. Stephenson, A. Robert, and G. Grübel, "X-ray spectroscopy: Revealing the atomic dance," Nat. Mater. **8**(9), 702–703 (2009).
[3]P. F. McMillan, "New materials from high-pressure experiment," Nat. Mater. **1**, 19–25 (2002).
[4]R. A. Graham, B. Morosin, E. L. Venturini, and M. J. Carr, "Materials modification and synthesis under high pressure shock compression," Rev. Mater. Sci. **16**(1), 315–341 (1986).
[5]W. J. Nellis, "Dynamic compression of materials: Metallization of fluid hydrogen at high pressures," Rep. Prog. Phys. **69**, 1479–1580 (2006).
[6]R. P. Drake and P. A. Norreys, "Focus on high energy density physics," New J. Phys. **16**(6), 065007 (2014).
[7]L. Dubrovinsky, N. Dubrovinskaia, O. Narygina, I. Kantor, A. Kuznetzov, V. B. Prakapenka, L. Vitos, B. Johansson, A. S. Mikhaylushkin, S. I. Simak, and I. A. Abrikosov, "Body-centered cubic iron-nickel alloy in Earth's core," Science **316**, 1880–1884 (2007).
[8]R. S. McWilliams, D. K. Spaulding, J. H. Eggert, P. M. Celliers, D. G. Hicks, R. F. Smith, G. W. Collins, and R. Jeanloz, "Phase transformations and metallization of magnesium oxide at high pressure and temperature," Science **338**, 1330–1333 (2012).
[9]D. Milathianaki, S. Boutet, G. J. Williams, A. Higginbotham, D. Ratner, A. E. Gleason, M. Messerschmidt, M. M. Seibert, D. C. Swift, P. Hering, J. Robinson, W. E. White, and J. S. Wark, "Femtosecond visualization of lattice dynamics in shock-compressed matter," Science **342**(6155), 220 (2013).
[10]G. Hammersley, L. A. Hackel, and F. Harris, "Surface prestressing to improve fatigue strength of components by laser shot peening," Opt. Lasers Eng. **34**(4–6), 327–337 (2000).
[11]R. Ernstorfer, M. Harb, C. T. Hebeisen, G. Sciaini, T. Dartigalongue, and R. J. D. Miller, "The formation of warm dense matter: Experimental evidence for electronic bond hardening in gold," Science **323**(5917), 1033–1037 (2009).
[12]J. Hohlfeld, S. Wellershoff, J. Gudde, U. Conrad, V. Jahnke, and E. Matthias, "Electron and lattice dynamics following optical excitation of metals," Chem. Phys. **251**, 237–258 (2000).
[13]M. Yokoo, N. Kawai, K. G. Nakamura, K. I. Kondo, Y. Tange, and T. Tsuchiya, "Ultrahigh-pressure scales for gold and platinum at pressures up to 550 GPa," Phys. Rev. B: Condens. Matter Mater. Phys. **80**(10), 104114 (2009).
[14]S. H. Shim, T. S. Duffy, and K. Takemura, "Equation of state of gold and its application to the phase boundaries near 660 km depth in Earth's mantle," Earth Planet. Sci. Lett. **203**(2), 729–739 (2002).
[15]T. Kenichi, "Evaluation of the hydrostaticity of a helium-pressure medium with powder x-ray diffraction techniques," J. Appl. Phys. **89**(1), 662–668 (2001).
[16]K. Tono, T. Togashi, Y. Inubushi, T. Sato, T. Katayama, K. Ogawa, H. Ohashi, H. Kimura, S. Takahashi, K. Takeshita, H. Tomizawa, S. Goto, T. Ishikawa, and M. Yabashi, "Beamline, experimental stations and photon beam diagnostics for the hard x-ray free electron laser of SACLA," New J. Phys. **15**, 083035 (2013).
[17]T. A. Pikuz, A. Y. Faenov, N. Ozaki, N. J. Hartley, B. Albertazzi, T. Matsuoka, K. Takahashi, H. Habara, S. Matsuyama, K. Yamauchi, R. Ochante, K. Sueda, O. Sakata, T. Sekine, T. Sato, Y. Umeda, T. Yabuuchi, T. Togashi, T. Katayama, M. Yabashi, M. Harmand, G. Morard, M. Koenig, V. Zhakhovsky, N. Inogamov, A. S. Safronova, A. Stafford, I. Y. Skobelev, S. A. Pikuz, T. Okuchi, Y. Seto, K. A. Tanaka, and R. Kodama, "Indirect monitoring shot-to-shot shock waves strength reproducibility during pump-probe experiments," J. Appl. Phys. **120**, 035901 (2016).
[18]A. L. Patterson, "The Scherrer formula for I-ray particle size determination," Phys. Rev. **56**, 978–982 (1939).
[19]P. Vinet, J. R. Smith, J. Ferrante, and J. H. Rose, "Temperature effects on the universal equation of state," Phys. Rev. B **35**(4), 1945 (1987).
[20]D. L. Heinz and R. Jeanloz, "The equation of state of the gold calibration standard," J. Appl. Phys. **55**(4), 885–893 (1984).
[21]E. G. Gamaly, "The physics of ultra-short laser interaction with solids at non-relativistic intensities," Phys. Rep. **508**(4–5), 91–243 (2011).
[22]S. Amoruso, N. N. Nedyalkov, X. Wang, G. Ausanio, R. Bruzzese, and P. A. Atanasov, "Ultrafast laser ablation of gold thin film targets," J. Appl. Phys. **110**(12), 124303 (2011).
[23]M. Nicoul, U. Shymanovich, A. Tarasevitch, D. von der Linde, and K. Sokolowski-Tinten, "Picosecond acoustic response of a laser-heated gold-film studied with time-resolved x-ray diffraction," Appl. Phys. Lett. **98**(19), 191902 (2011).
[24]T. G. White, P. Mabey, D. O. Gericke, N. J. Hartley, H. W. Doyle, D. Mcgonegle, D. Rackstraw, A. Higginbotham, and G. Gregori, "Electron-ion equilibration in laser heated gold films," Phys. Rev. B **90**(1), 014305 (2014).
[25]B. C. Stuart, M. D. Feit, S. Herman, A. M. Rubenchik, B. W. Shore, and M. D. Perry, "Optical ablation by high-power short-pulse lasers," J. Opt. Soc. Am. B **13**(2), 459 (1996).
[26]T. Tsuchiya, "First-principles prediction of the P-V-T equation of state of gold and the 660-km discontinuity in Earth's mantle," J. Geophys. Res. **108**, 1–9, doi:10.1029/2003JB002446 (2003).